



Identification of time-dependent interfacial mechanical properties of adhesive by hybrid/inverse method

J. Wang^a, Y.L. Kang^{a,*}, Q.H. Qin^b, D.H. Fu^a, X.Q. Li^a

^a Department of Mechanics, Tianjin University, Tianjin 300072, PR China

^b Department of Engineering, Australian National University, Canberra, ACT 0200, Australia

ARTICLE INFO

Article history:

Received 12 December 2007

Received in revised form 5 March 2008

Accepted 7 March 2008

Available online 22 April 2008

PACS:

46.35.+z

02.30.Zz

68.35.Np

07.05.Tp

07.05.Fb

Keywords:

Viscoelasticity

Hybrid/inverse identification method

Time-dependent interfacial parameters

Interfacial adhesive experiment

Numerical simulation

Genetic algorithm

ABSTRACT

Interfacial mechanical properties of the adhesive bonded interface are strongly time-dependent in most engineering structures due to the viscoelasticity of the adhesive layer. To predict those properties and investigate their effect on the time-dependent adhesive structures, a novel hybrid/inverse identification method is developed in this paper. The method is made up of an optimization technique coupled with a new time-dependent interfacial adhesive model, the interfacial adhesive experiment at various loading rates and the finite element numerical simulation. Based on the interfacial failure results obtained from experiment and the numerical simulation, the hybrid/inverse identifying procedure time-dependent interfacial parameters is constructed by means of genetic algorithms and the time-dependent interfacial adhesive parameters can then determined. In end an independent experiment is presented to verify the reasonableness of the values of the interfacial parameters. The hybrid/inverse identification method is proved to be promising in identifying time-dependent interfacial parameters of adhesive bonded structures.

© 2008 Elsevier B.V. All rights reserved.

1. Introduction

Adhesive bonding is a modern assembly technique where two similar or non-similar materials are joined using an adhesive. Its major advantages over traditional assembly techniques like bolting, screwing, welding and soldering are (1) relative uniform stress distribution; (2) ability to bond dissimilar as well as similar materials including metals, plastics, elastomers, glass, ceramics and wood; (3) clean-looking joints; (4) less critical tolerances acceptable for high performance bonding compared to mechanical fastening methods; and (5) superior thermal resistance. These advantages make it becomes an important part of manufacturing, not only in the aerospace industry but also in the automotive, wood-based panel, and marine industries in recent years. It has been recognized that interfacial properties of adhesive joints have a strong influence on the performance and reliability of the whole structures. During the past decades, various interfacial theories and models have been developed to study the mechanical perfor-

mance of composite interfaces. Needleman [1] introduced a cohesive concept into computational mechanical framework and presented an interface potential that specifies the dependence of the interface tractions upon the interface separation. Tvergaard and Hutchinson [2] used a traction-separation law to model the fracture process ahead of the crack-tip in an interfacial structure. The damage and debonding behavior of interfaces were investigated using the interfacial fracture and its failure criteria presented in [3–6]. Based on the supposition principle time-dependent fields, Schapery [7] developed an interfacial model which combines a viscoelastic constitutive equation with a damage function. More approaches incorporating time effects into material separation interfacial models can also be found in [8–10]. There is, however, very few work reported on interfacial mechanical characteristics by combining the direct experimental method and numerical simulation. Perhaps this is due to difficulties in conducting experiments on complex interfacial properties. Lin et al. [11] investigated interfacial properties of a real metal matrix composite Al6061–10%Al₂O₃ based on the results obtained from experiment and the non-continuum four-node interface model. Xu et al. [12] calibrated the rate-dependent cohesive zone parameters by

* Corresponding author. Tel./fax: +86 22 27403610.

E-mail address: tju_ylkang@yahoo.com.cn (Y.L. Kang).

comparing a series of numerical simulations with experimental curves to describe the crack growth in a thermoplastic adhesive. To the authors' knowledge, there is no report on identifying time-dependent interfacial properties of adhesive structures by using integrated approach of experimental and numerical simulation.

In this paper, a new hybrid/inverse identification method is proposed to identify time-dependent interfacial parameters in adhesive structures. The method is constructed by integrating a newly developed time-dependent interfacial adhesive model, numerical simulations and optimization process, and interfacial experiments at various loading rates. The optimization process was conducted based on a reasonable objective function representing the difference between numerical prediction and experimental observation. A experimental example is used to verify the applicability of the proposed identification algorithm.

2. Hybrid/inverse identification method

Hybrid technique, i.e., a combination of theory and experiment, has been widely applied in designing and analyzing realistic models of engineering events. Applications of hybrid-technique to 2- and 3-dimensional problems with dissimilar materials have been reported by Laermann [13,14] and Kobayashi [15]. Typically, hybrid/inverse identification method is an inverse method which integrates the numerical simulation and experimental analysis into one system. This method is made up of an optimization technique coupled with the experimental measurement and the FEM simulation. The finite element analysis is based on a newly proposed time-dependent interface element model. First, a set of unknown parameters related to interfacial strength and damage are defined and selected as objective parameters to be identified. A finite element model incorporating the time-dependent interface element is then developed and used to search for an approximate solution which has a minimum difference to the corresponding experimen-

tal results. With the algorithm, the process of identifying interfacial parameters is a process to compare the numerical results obtained with the experimental results and to minimize their difference. Fig. 1 illustrates the flow-chart of the hybrid identification algorithm.

2.1. The time-dependent interfacial adhesive model

The time-dependent interfacial model developed here follows the work of Needleman [1]. The model was derived based on Kelvin model (see Fig. 2) which consists of a time-independent cohesive zone model and a dashpot is placed parallel to the zone model.

In this work, normal material separation is considered only. Thus, the Kelvin model for the case of uniaxial constitutive relationship [16] between stress and strain becomes

$$\sigma = E\epsilon + \eta\dot{\epsilon} \quad (1)$$

The corresponding constitutive equation of the time-dependent interfacial model can then be written as

$$T_n = \tilde{T}_n + \eta_n \frac{d\Delta_n}{dt} \quad (2)$$

where \tilde{T}_n is the time-independent cohesive traction which can be obtained using the cohesive law of the interfacial model (spring element) [1]

$$\tilde{T}_n = -\tilde{\sigma}_{max} z e^{\frac{\Delta_n}{\delta_{nc}}} \exp\left(-z \frac{\Delta_n}{\delta_{nc}}\right) \quad (\Delta_n \leq \delta_{nc}) \quad (3)$$

$$\tilde{T}_n = 0 \quad (\Delta_n > \delta_{nc}) \quad (4)$$

where z is $16e/9$, e is $\exp(1)$; $\tilde{\sigma}_{max}$ is the cohesive strength and δ_{nc} is the critical opening displacement. The structure (see Fig. 2) is assumed to be broken when the normal displacement jump Δ_n reaches δ_{nc} . The hat over the cohesive zone quantities indicates time-independent parameters which are different from the

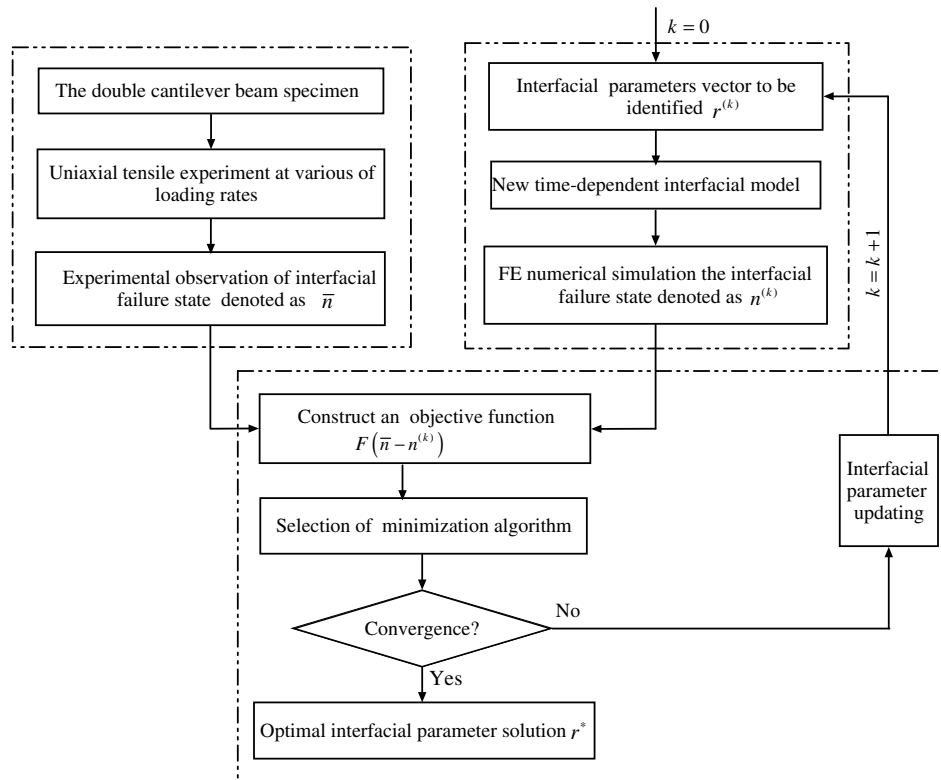


Fig. 1. Flow-chart of hybrid/inverse identification method.

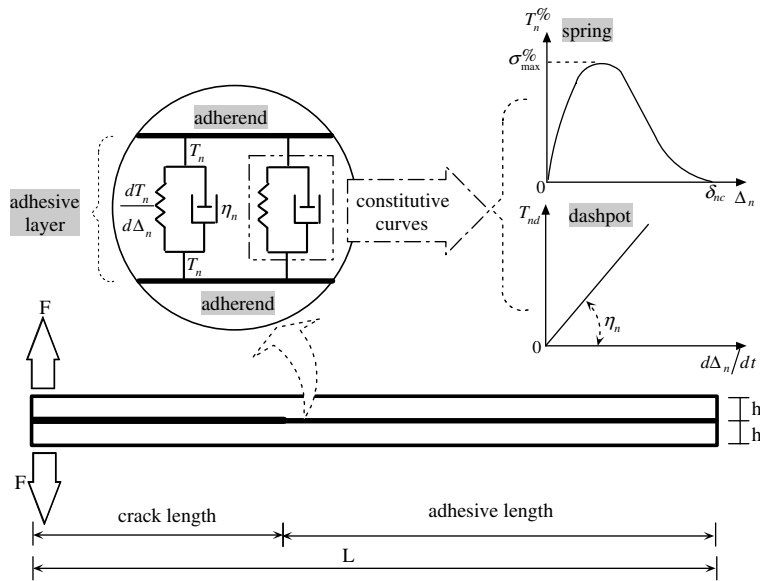


Fig. 2. The time-dependent interface model and the double cantilever beam specimen.

time-dependent ones. It should be mentioned that Eq. (2) is obtained based on the following three assumptions: (1) the stiffness of the time-independent cohesive zone model was used to replace E in the Kelvin model; (2) the displacement jump across the cohesive zone and the cohesive surface traction were used to replace strain and stress in the Kelvin model; and (3) a constant η_n with a unit of force per velocity per area (dashpot coefficient per area) was used to replace η with a unit of force per strain rate per area (viscosity) in the Kelvin model.

It is obvious from Eq. (2) that there are three interfacial parameters to be identified. They are interfacial strength limit $\bar{\sigma}_{\max}$, tensile separation limit δ_{nc} , and viscosity coefficient η_n .

2.2. Uniaxial tensile experiment for adhesive DCB at various loading rates

The design of the experiment component is critical in the proposed hybrid inverse method. The experimental results needed for the identification are obtained from a reasonable data measurement. It should be mentioned that the whole process of the experiment is time-dependent and the corresponding results are obtained in real time measurement. In the experiment, a video-recorded image acquisition system is adopted to record the history of the applied load and displacement and the local interfacial deformation. The experiment conducted in this work is a uniaxial tensile test on a double cantilever beam (DCB) at various loading rates. The measurement of mechanical performance of DCB adhesive specimen is conducted in accordance with ASTM D3433 standard [17]. The aluminum alloy (LY12-CZ) adherens (Young's modulus $E = 71$ GPa, Poisson's ratio $\nu = 0.33$) is bonded by the silica gel adhesive (WL-506). And a cohesive crack-like defect was obtained at the beginning of the bonding process by placing a Teflon tape at the mid-thickness of the adhesive layer.

The loading of the specimen was carried out in an Instron 3343 electromechanical testing machine. A grid technique was adapted to measure displacement fields around the interface of the model. In order to accurately record the images of the interfacial deformation, uniform marker lines were printed on the surface of the interface of the adherens (Fig. 3). When the specimen was loaded with different constant displacement rates at the load-point, the load vs. load-point displacement curves and video-recorded images of the interfacial deformation through the marker lines were recorded

by computerized data acquisition system and a microscope linked to a CCD (basler A202k), respectively. The configuration of the loading setup is shown in Fig. 3.

The load vs. load-point displacement curves for the DCB adhesive specimen under constant load-point displacement rates of $v = 0.02, 0.2, 1.0$ and 2.0 mm/s, respectively, are presented in Fig. 4. It can be seen from Fig. 4 that the maximal load increases from 36.4 N to 43.9 N, along with the increase in the level of loading velocity from 0.02–2.0 mm/s. And the corresponding displacements increase also from 2.64–3.20 mm. Therefore an increase in the loading velocity leads to an increase in the cohesive energy of the time-dependent adhesives.

2.3. Numerical simulation and identification of the time-dependent interfacial parameters

In this section, the interfacial failure of the adherens sample is numerically simulated using the finite element package ABAQUS [18]. In the forward calculations, the adherens material parameters are exactly identical to those of the actual materials mentioned in the experiments. The four-node bilinear element is used to model the adherens and the size of the elements was gradually increased with increasing distance from the interfacial elements. To model interfacial separation, several time-dependent interfacial adhesive elements are placed along the interface whose thickness is assumed to be 0.2 mm, where the two nodes of the interfacial elements are initially coincident. At the early loading stage of the DCB specimen, the stresses between the two nodes of the interfacial elements increase steeply. As the stress reaches its maximum, the two nodes begin to separate with a reducing stress. At the point of the critical separation, the interfacial stress drops to zero. Thus, the interfacial element is effectively terminated and removed, and the damage propagates at the interfacial adhesive region. The proposed interfacial element has been integrated into ABAQUS via its user-defined subroutine (UEL) capability.

It is noted that the key point in formulating the inverse problem as an optimization problem is to construct a proper objective function F . To this end, an objective function is constructed based difference of the results obtained from the experiment and FEM simulation. The results of failure region and failure mode of the interface are used as basic decision variables in the objective

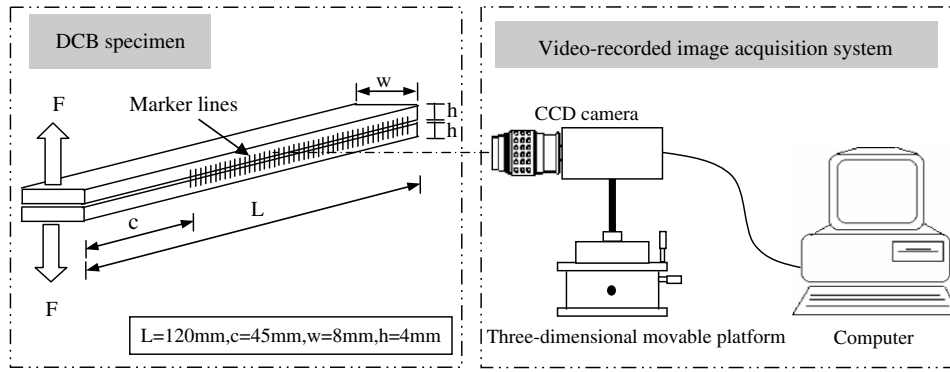


Fig. 3. DCB specimen and video-recorded image acquisition system.

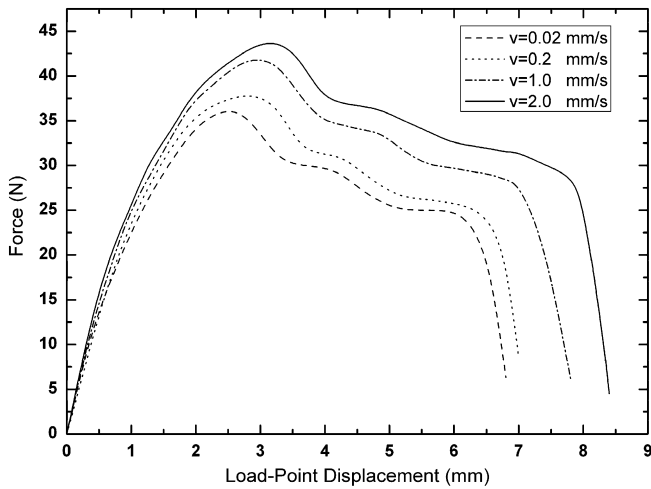


Fig. 4. Force vs. load-point displacement curves at different rates.

function. The construction of the proposed objective function is detailed below.

For the dynamic process of the interfacial tensile deformation, suppose there are s interface elements in FE analysis along the interface under consideration. Each element of the interface is denoted by a number i ($i = 1, 2, \dots, s$). Assume that the failure state of each element is characterized by two variables n_i and \bar{n}_i ($i = 1, 2, \dots, s$), which represent the failure of the i th element in the FE calculation and the experimental observation, respectively. The values of n_i and \bar{n}_i are determined in the following way: (1) in the FE forward simulation, $n_i(r, t) = 0$ if the tensile failure occurs, otherwise $n_i(r, t) = 1$; (2) in the results of experiments, $\bar{n}_i(t) = 0$ represents the actual tensile failure state of the interfacial element, otherwise $\bar{n}_i(t) = 1$. And then, a function $\Theta(n_i, \bar{n}_i)$ is proposed to show whether the failure mode from the FE simulation of the i th element coincides with that from the video-recorded images during the experiment at the same time. If $n_i(r, t) = \bar{n}_i(t)$, the function $\Theta(n_i(r, t), \bar{n}_i(t)) = 0$ otherwise $\Theta(n_i(r, t), \bar{n}_i(t)) = 1$. Based on the analysis above, the objective function is defined as

$$F(r) = \sum_{t=1}^q \sum_{i=1}^s \Theta[n_i(r, t), \bar{n}_i(t)] \quad (5)$$

where q represents the time period used in numerical calculation, which is taken to be the same as that in the actual experiment process and r is a vector dependent on the time-dependent interfacial parameter $\bar{\sigma}_{\max}, \delta_{nc}, \eta_n$. With the objective function (5), the present inverse problem can be regarded as a problem of finding an optimal

Table 1

Search range of interfacial parameters based on time-dependent CZM

Interfacial parameters	$\bar{\sigma}_{\max}$ (MPa)	δ_{nc} (mm)	η_n (MPa s/mm)
Search range	0 ~ 200	0.00 ~ 2.00	0 ~ 200

point r^* in the three-dimensional space $R(\bar{\sigma}_{\max}, \delta_{nc}, \eta_n)$ where the function $F(r)$ is minimized by the corresponding results of FE simulation calculation coincide with that observed from the experiment. Thus, the solution of the inverse problem can be given as

$$r^* = \arg \min_{r \in R} F(r) \quad (6)$$

It can be seen from Eq. (5) that the objective function $F(r)$ is a discrete function. It is, therefore, very difficult to evaluate the derivative of the function $F(r)$, which is required in the gradient-based search method. To bypass this problem genetic algorithm (GA) is employed in this work as only the objective function itself is required in GA. In addition to derivatives of the objective function being not required, GA has also many other advantages over the traditional optimization techniques including working on the codes of the variables to be optimized, searching with multi-point parallel method, adopting probability search technique and performing with only objective function information [19]. Moreover, GA is a stochastic global search technique and can work well on a population of points in the search space for each generation. In our analysis, parameters used in GA calculation are as follows: the population size of each generation is set to be 30; the probabilities of crossover and mutation are taken as 0.8 and 0.05, respectively; and the maximum generation is set to be 100. It should be mentioned that the initial population of chromosomes is randomly generated within a prescribed search space, as show in Table 1.

3. Identification results and discussion

The identification of time-dependent interfacial parameters of the adhesive structure is performed based on the results of the DCB experiments at the loading rate of $v = 2.0$ mm/s. With this loading rate, the corresponding identification values of the three interfacial parameters in the time-dependent adhesive interfacial model are: Strength limit $\bar{\sigma}_{\max} = 8.1$ MPa, tensile separation limit $\delta_{nc} = 0.35$ mm, and viscosity coefficient $\eta_n = 15.2$ MPa s/mm. It can be seen from the identification results that the interface between the aluminum alloys is a time-dependent weakly bonded interface and the strength limit is much lower than the strength of the aluminum alloy. Thus, the failure is easier to occur at the adhesive interface due to the relatively low interfacial strength when the adhesive bonding is in service.

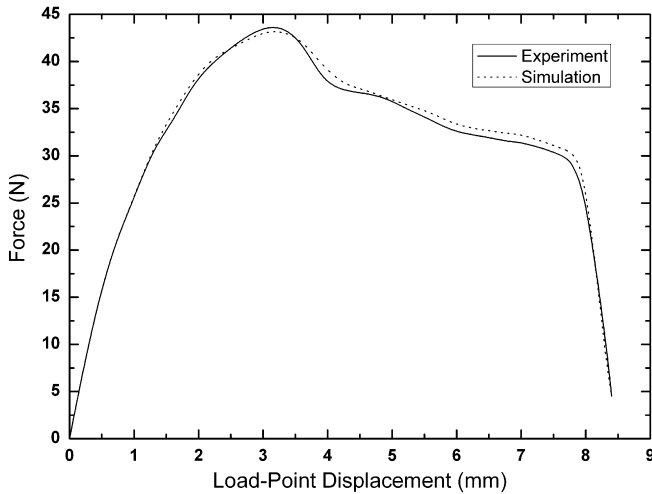


Fig. 5. Force vs. load-point displacement curves of FE simulation and experiment at $v = 2$ mm/s.

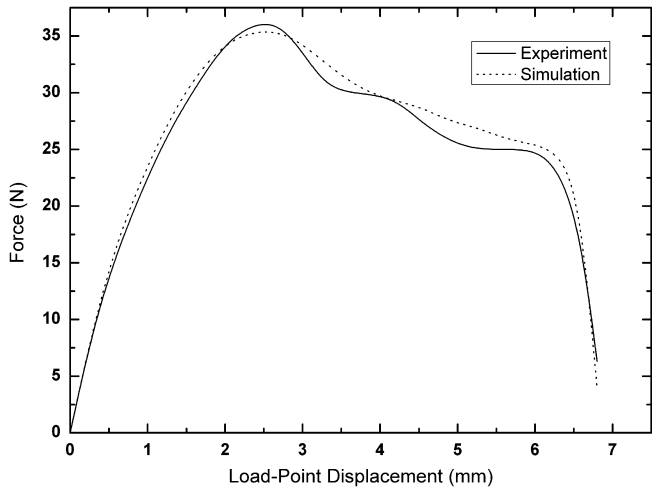


Fig. 6. Force vs. load-point displacement curves of FE simulation and experiment at $v = 0.02$ mm/s.

To improve the robustness of the identification procedure, failure region and failure mode at the interface in real time during the whole process of the experiment are compared with the numerical simulation results under the same loading rate. Furthermore, it is important to ensure that the inverse solution obtained is physically meaningful. To this end, two kind of experimental verification methods are adopted. The first one is the self verification, i.e., the comparison is performed between the experimental results at a given loading rate ($v = 2$ mm/s) and the corresponding numerical simulation prediction with the interfacial parameters identified based on the experiment at the same loading rate. The second is the independent verification, i.e., the results of numerical simulation based on the interfacial parameters identified above are com-

pared with the results of another independent experiment at the lower loading rate ($v = 0.02$ mm/s). The records of force vs. load-point displacement curves which are the general response of the specimen during the experiments are depicted in Figs. 5 and 6. By comparing the results of the numerical simulations with those of experiments, the force vs. load-point displacement curves are good matched. Thus, the proposed hybrid/inverse identification method is well-posed and the inversion results of the interfacial parameters based on the time-dependent adhesive interfacial model is reliable.

4. Conclusions

Based on the proposed time-dependent interfacial adhesive model, a hybrid/inverse identification method has been developed and used to analyze the time-dependent interfacial adhesive properties in adhesive bonded structures. Using this method, the interfacial parameters such as the strength, stiffness and the viscosity coefficient of the adhesive interface are quantitatively identified. Further, an independent experiment is presented to verify the reasonableness of the values of the interfacial parameters. The proposed method is proven to be promising in solving time-dependent inverse problems of actual structures with multiple unknown interfacial parameters.

Acknowledgements

The authors would like to thank Professor K.H. Laermann (Bergische Universität-GH Wuppertal, D-42285 Wuppertal, Germany) for his useful discussion in hybrid/inverse method and also would like to acknowledge the support from the National Science Foundation of China (Nos. 10572102) and National Basic Research Program of China (973 Program) (Nos. 2007CB714001 and 2007CB714002).

References

- [1] A. Needleman, *J. Appl. Mech.* 54 (1987) 525–531.
- [2] V. Tvergaard, J.W. Hutchinson, *J. Mech. Phys. Solids* 41 (1993) 1119–1135.
- [3] O. Allix, P. Ladeveze, *Compos. Struct.* 22 (1992) 235–242.
- [4] X.P. Xu, A. Needleman, *Int. J. Fract.* 74 (1996) 289–324.
- [5] O. Chabanet, D. Steglich, J. Besson, V. Heitmann, *Comput. Mater. Sci.* 26 (2003) 1–12.
- [6] J.L. Wang, *Int. J. Solids Struct.* 43 (2006) 6630–6648.
- [7] R.A. Schapery, *Int. J. Fract.* 97 (1999) 33–66.
- [8] Z.P. Bazant, Y.N. Li, *Int. J. Fract.* 86 (1997) 247–265.
- [9] C.M. Landis, T. Pradoen, J.W. Hutchinson, *Mech. Mater.* 32 (2000) 663–678.
- [10] C. Xu, T. Siegmund, K. Ramani, *Int. J. Adhes. Adhes.* 23 (2003) 9–13.
- [11] X.H. Lin, Y.L. Kang, Q.H. Qin, D.H. Fu, *Comput. Mater. Sci.* 32 (2005) 47–56.
- [12] C. Xu, T. Siegmund, K. Ramani, *Int. J. Adhes. Adhes.* 23 (2003) 15–22.
- [13] K.H. Laermann, *Exp. Mech.* 21 (1981) 386–388.
- [14] K.H. Laermann, *Opt. Lasers Eng.* 32 (1999) 183–203.
- [15] A.S. Kobayashi, *Exp. Mech.* 23 (1983) 338–347.
- [16] Y.T. Zhang, *Theory of Thermo-viscoelasticity*, Publishing Company of Tianjin's University, Tianjin, 2002 [in Chinese].
- [17] Anon., ASTM D3433-Standard test method for fracture strength in cleavage of adhesives in bonded metal joints. American Society for Testing and Material, Philadelphia, PA, USA, 1999 (Reapproved 2005).
- [18] ABAQUS/Standard User's Manual for Version 6.2, vol. I, II and III, Hibbitt, Karlsson & Sorensen, Inc., 2001.
- [19] K.F. Man, K.S. Tang, S. Kwong, *Genetic Algorithms: Concepts and Designs*, Springer Verlag, London, 1999.